STRUCTURAL BIOLOGY

Volume 79 (2023)

Supporting information for article:

Structural insights into the substrate specificity and activity of a novel mannose 2-epimerase from *Runella slithyformis*

Hang Hang, Xiaomei Sun, Wataru Saburi, Saki Hashiguchi, Jian Yu, Toyoyuki Ose, Haruhide Mori and Min Yao

Table S1 The primers used for construction of mutants of *Rs*ME.

Primers	Sequences (5′ →3′)
W251A_F	GCTGGGTGGGATCGCTTCAATCC
W251A_R	AACGATGTCAAATTTGATCTGAGGAG
W251F_F	TTCGGGTGGGATCGCTTCAATCC
W251F_R	AACGATGTCAAATTTGATCTGAGGAG
D254A_F	CGCTTCAATCCCGATGGTC
D254A_R	AGCCCACCCCCAAACGATGTC

Figure S1 Structural superimposition of *Se*SQI (A) and *Rm*CE (B). (A)The apo form and substrate complex of *Se*SQI were showed in light blue and orange, respectively. The bound substrate sulfofructose (SF) is represented as green sticks. The conformational changes in *Se*SQI are indicated by black dashed ellipses and black arrows. (B)The apo and substrate complex of *Rm*CE were colored pink and yellow. The bound substrate 4-O-β-D-glucosyl- D -mannose were represented as limon sticks. The loop $_{\alpha7-\alpha8}$ and loop $_{\alpha11-\alpha12}$ are indicated as black arrows. The residue W385 of loop $_{\alpha11-\alpha12}$ are shown as sticks.

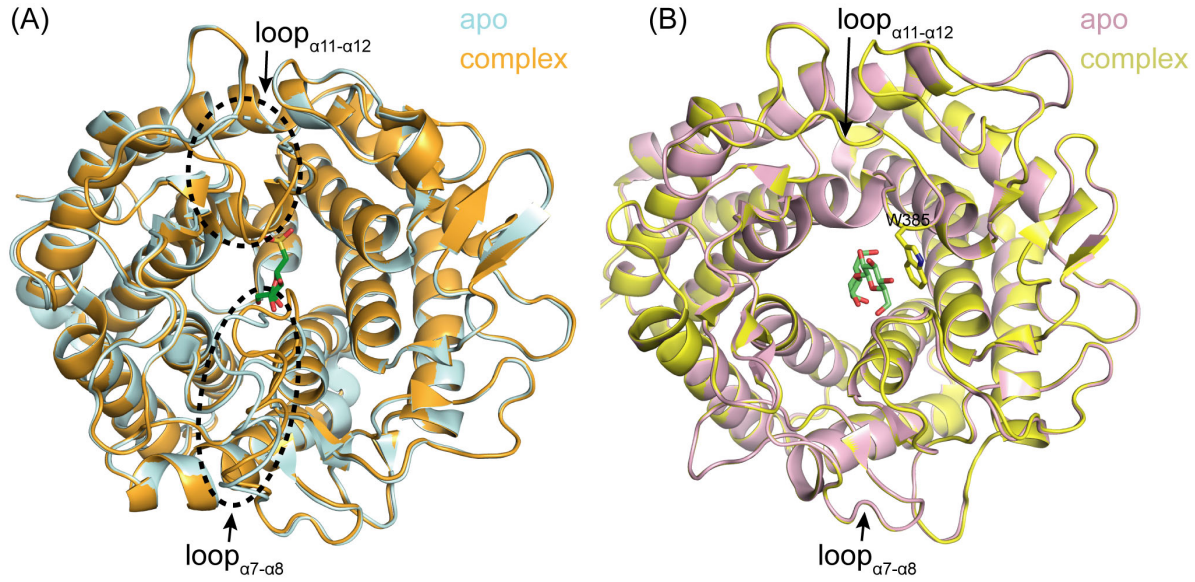

Figure S2 Multiple sequence alignment of AGE family members. *Df*ME, *Dyadobacter fermentans* ME (Uniprot No., C6VWU2); *Bt*CE, *Bacillus thermoamylovorans* CE (Uniprot No., A0A0D0GHZ5); *Ra*CE, *Ruminococcus albus* CE (Uniprot No., P0DKY4), *Rm*CE, *Rhodothermus marinus* CE (Uniprot No., F8WRK9); *Cs*CE, *Caldicellulosiruptor saccharolyticus* CE (Uniprot No., A4XGA6); *St*CE, *Spirochaeta thermophila* CE (Uniprot No., E0RU15); *Mm*MI, *Marinomonas mediterranea* MI (Uniprot No., F2JVT6); *Xf*AGE, *Xylella fastidiosa* (Uniprot No., B2I5L9); *n*AGE, *Nostoc sp. KVJ10* AGE (Uniprot No., A0A452CSU8); *Ss*AGE, *Sus scrofa* AGE (Uniprot No., P17560); *a*AGE, *Anabaena sp. CH1* (Uniprot No., A4UA16); *Se*SQI, *Salmonella typhimurium* SQI (Uniprot No., Q8ZKT7); and *Ec*SQI, *Escherichia coli* SQI (Uniprot No., P32140). Sequence alignments were performed with T-Cofee and visualized with Espript. The key catalytic residues are marked with a blue pentagram. The secondary structural elements of *Rs*ME are shown at the top of the alignment.

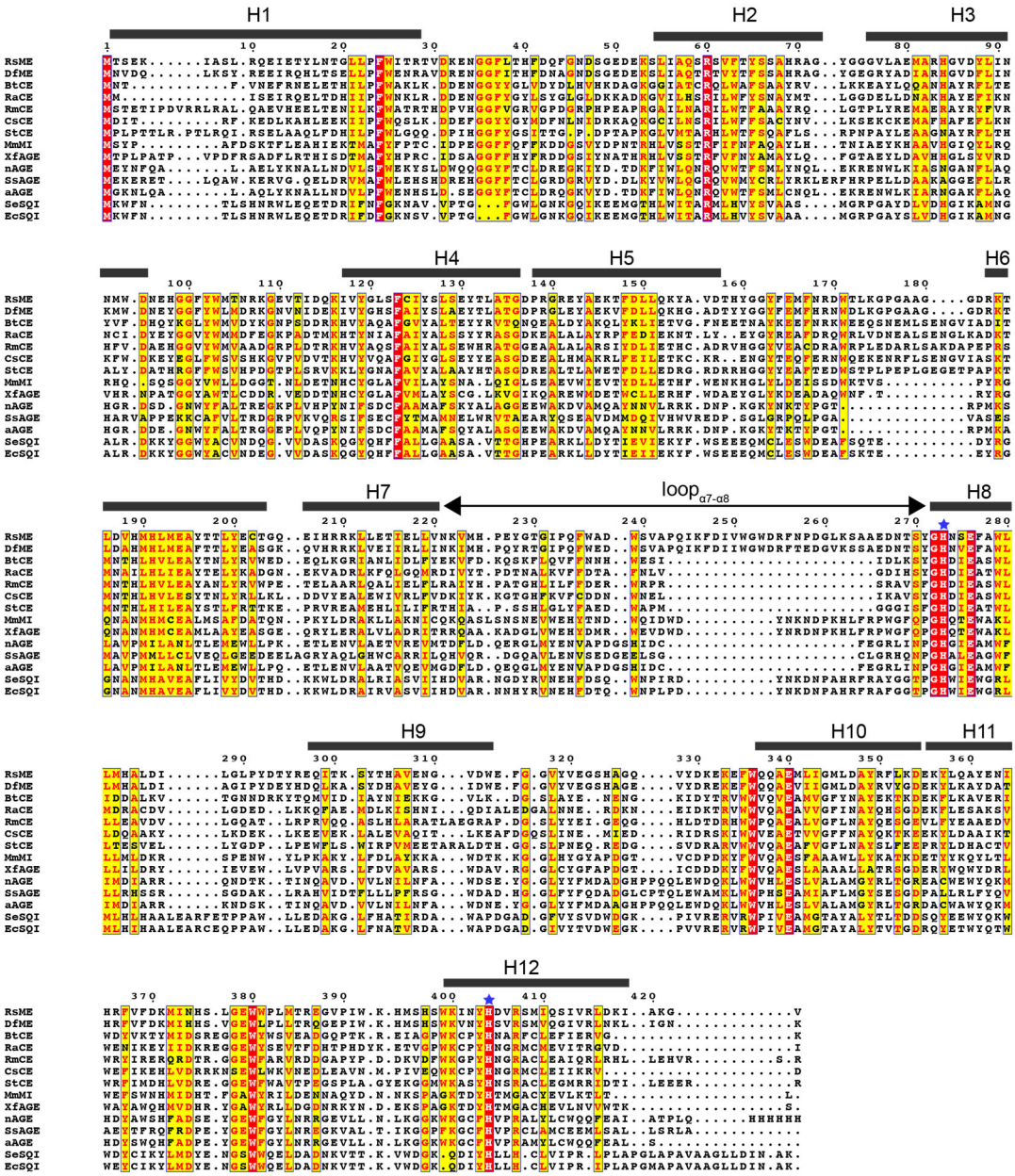
H1
H2
H3
H4
H5
H6
H7
loop α7-α8
H8
H9
H10
H11
H12
RsME
DfME
BtCE
RaCE
RmCE
CsCE
StCE
MmMI
XfAGE
nAGE
SsAGE
aAGE
SeSQI
EcSQI

Figure S3 Superposition of the structure of substrate-free *Rs*ME (cyan) with other AGE members. *Asp*AGE (orange), *Rm*CE (yellow), *Mm*MI (violet), and *Ec*SQI (pale green). The loop$_{\alpha7-\alpha8}$ is highlighted. The binding pocket is indicated by a dashed black oval.

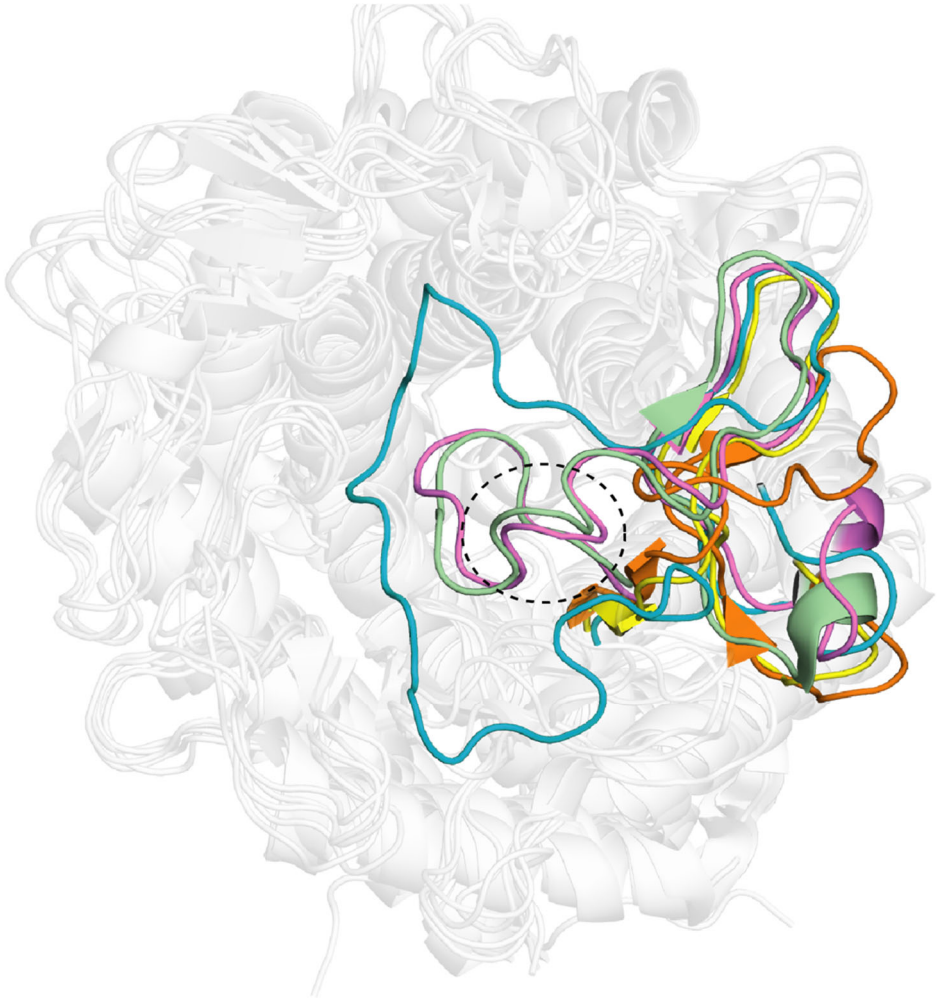

Figure S4 Close-up view of the active site. The residues surrounding the glycerol molecules are shown as sticks. Hydrogen bonds are indicated by dashed lines. The omit map of glycerol is countered at 3.0 σ and shown as a brown mesh.

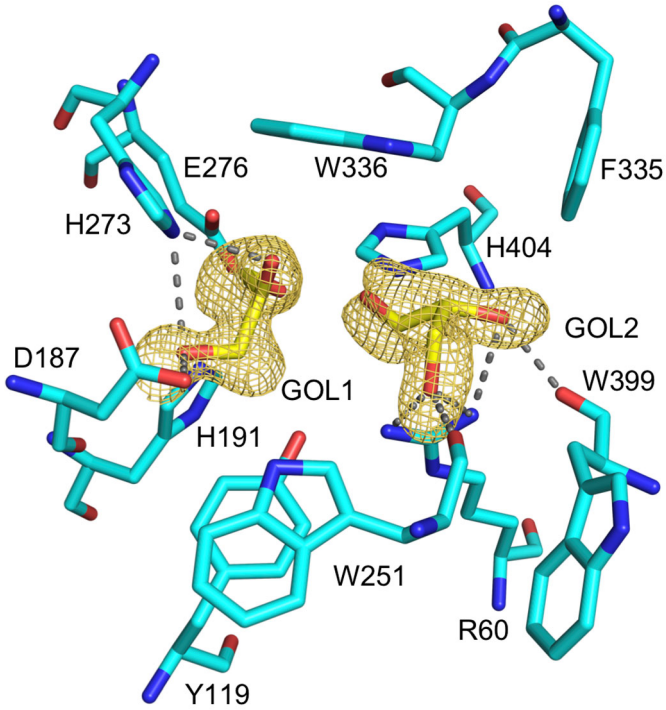

Figure S5 (A) Chemical reaction of C2 hydroxyl epimerization catalysed by *Rs*ME. (B) Chemical structure of the intermediate analog D-glucitol.

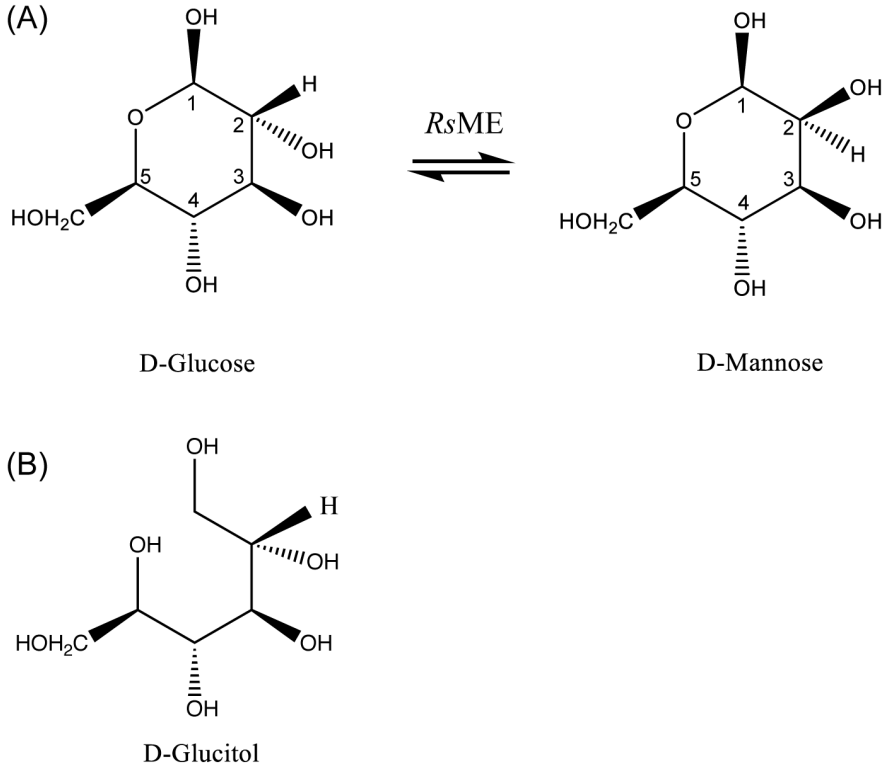

Figure S6 Loopα7-α8 alignment of the apo form (cyan) and the D-glucitol binding form (light blue).

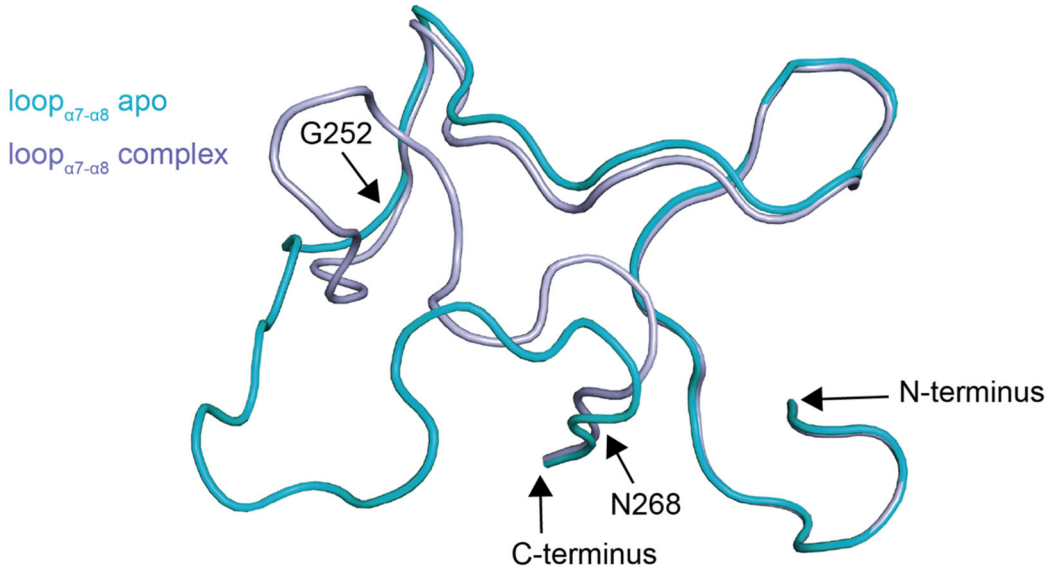

Figure S7 Hydrogen bond networks of D187 in *Rs*ME (A) and the corresponding residue N196 in *Rm*CE (B). The hydrogen bonds are indicated by black dashed lines.

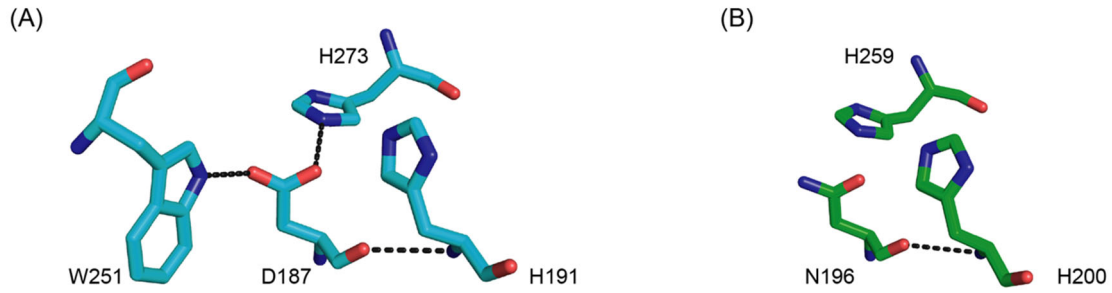

Figure S8 Docking models of *Rs*ME with D-glucose and D-mannose. (A) The initial structures of *Rs*ME and ligands molecules (D-glucose, and D-mannose). The predicted binding site is indicated by a black square. (B) Close-up of the binding site of D-glucose in *Rs*ME. (C) Close-up of the binding site of D-mannose in *Rs*ME. Possible hydrogen bonds between the ligand and *Rs*ME are shown as black dashed lines.

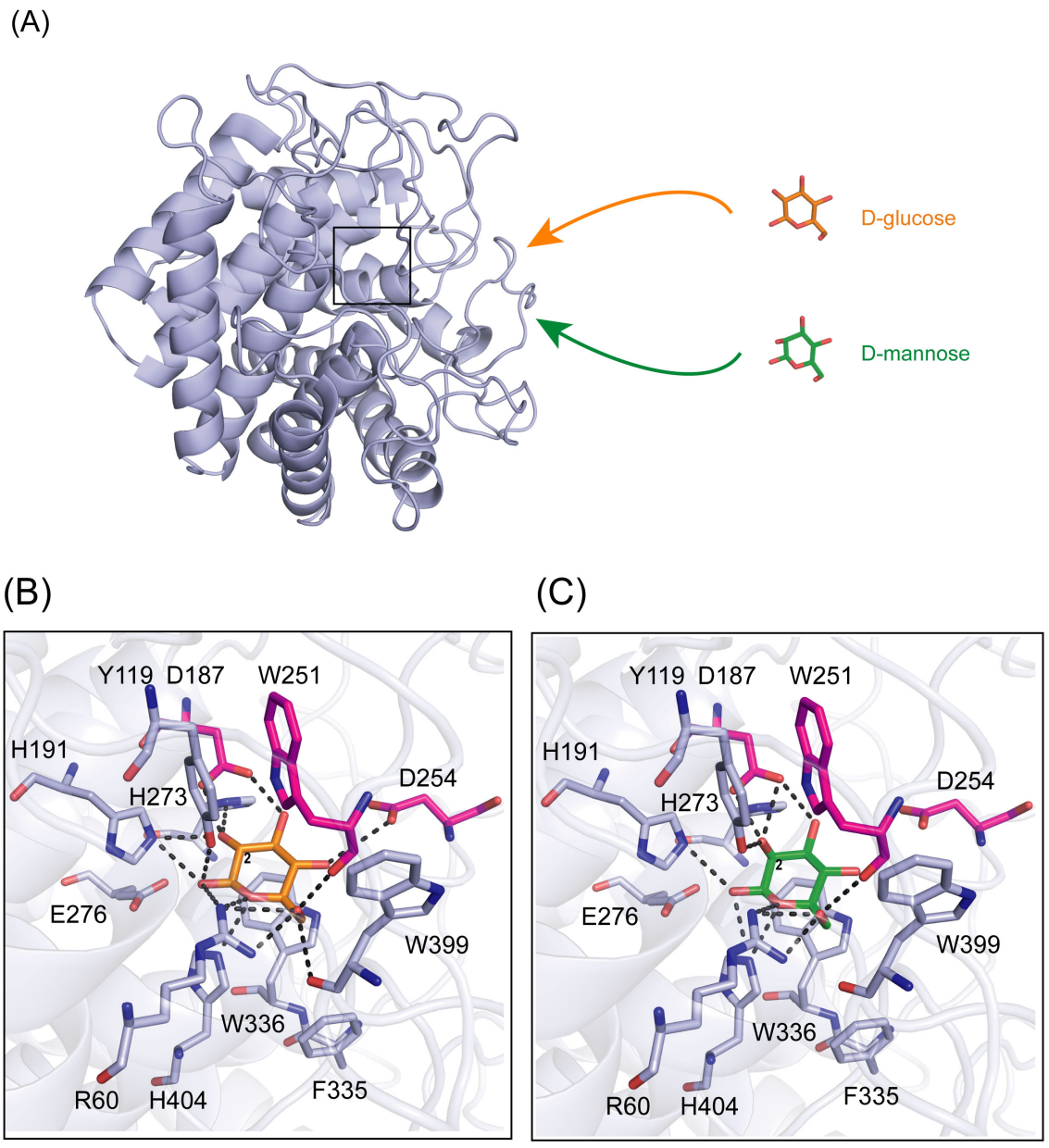

Figure S9 Superimposition of the docking model of *Rs*ME_D-mannose with *Rm*CE_4-*O*-β-D-glucosyl-D-mannose. The *Rs*ME and *Rm*CE are shown in cartoon representation as light blue and light grey, respectively. 4-*O*-β-D-Glucosyl-D-mannose is represented as cyan sticks. The enlarged image shows the residues interacting with the ligand of *Rs*ME. The residues specific to *Rs*ME are colored magenta.

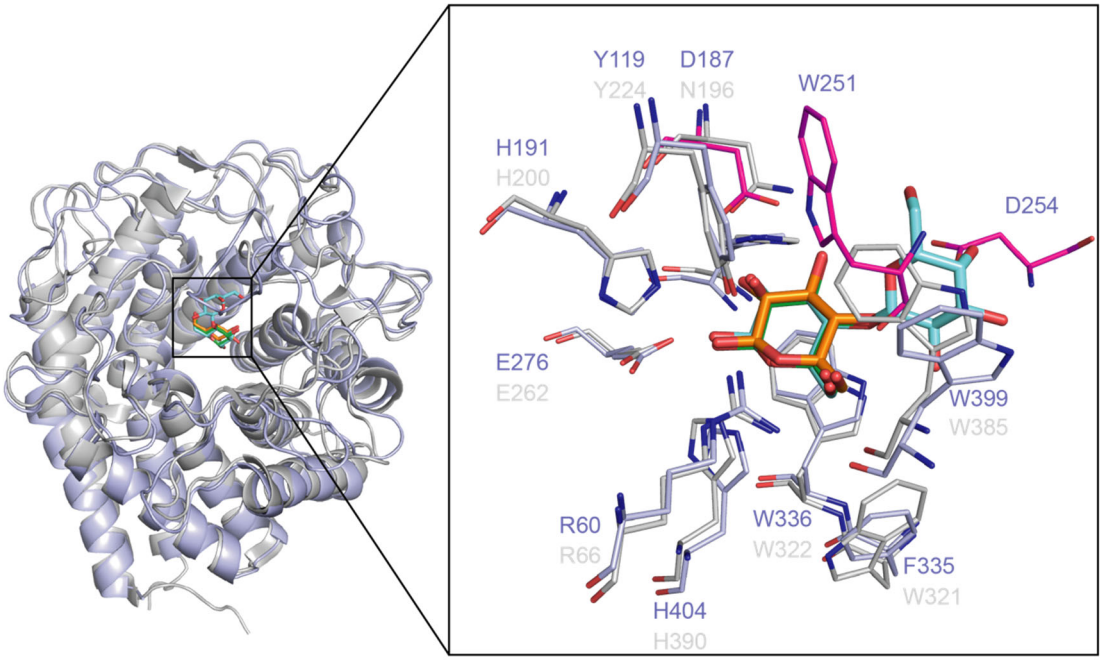

Figure S10 Structure of *Rs*ME(D254A)_D-glucitol. (A) 2D diagram of D-glucitol interaction with *Rs*ME(D254A). Hydrogen bonds are represented by green and black (for active residues) dashed lines, and hydrophobic contacts are shown as light orange circular arcs. (B)Superimposition of the active pocket between *Rs*ME(D254) (gray) and *Rs*ME(D254A)_D-glucitol (orange).

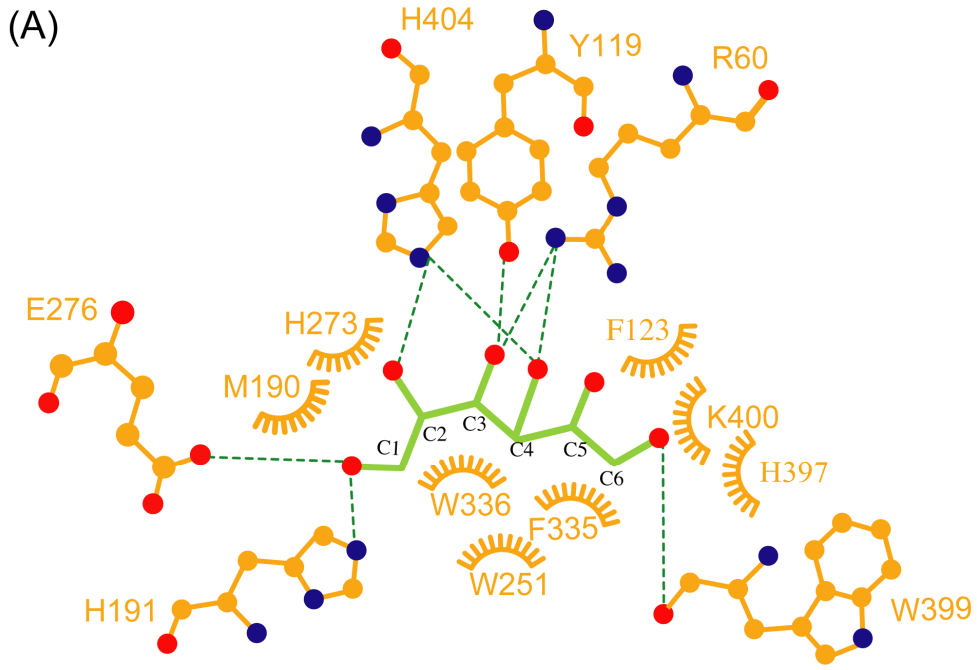

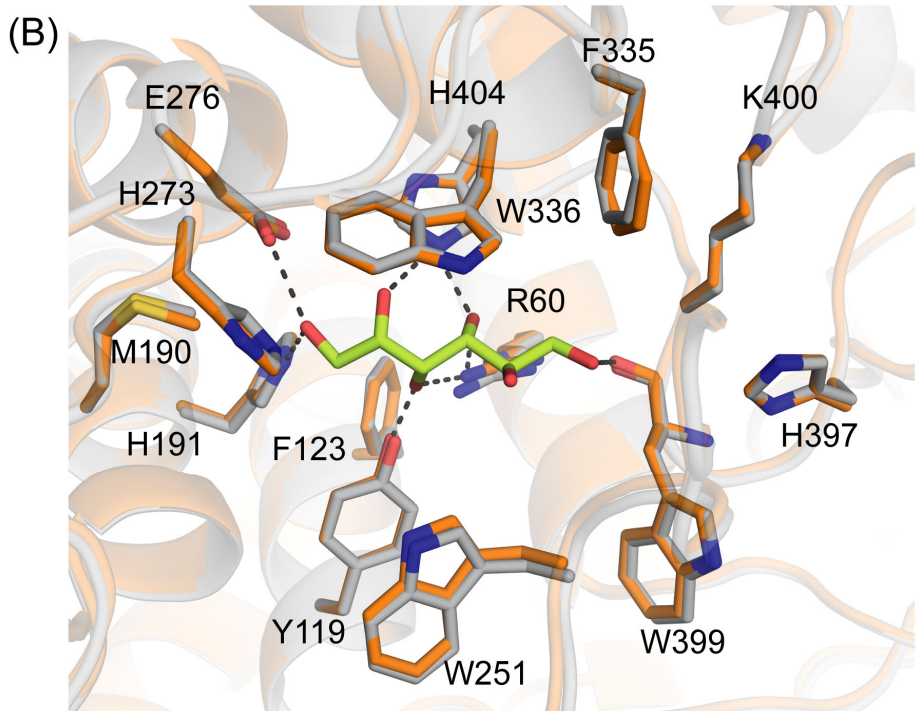

Figure S11 Structure alignment of *Se*SQI with *Rm*CE. (A) Structure superposition of *Se*SQI_SF (pink) with *Rm*CE-cellobiitol (yellow). (B) A close-up view of the steric hindrance of non-reducing end sugar residue with loop α7–α8 of *Se*SQI. The cellobiitol is shown as spheres. The residues R238-F239 of loop α7–α8 are colored red.

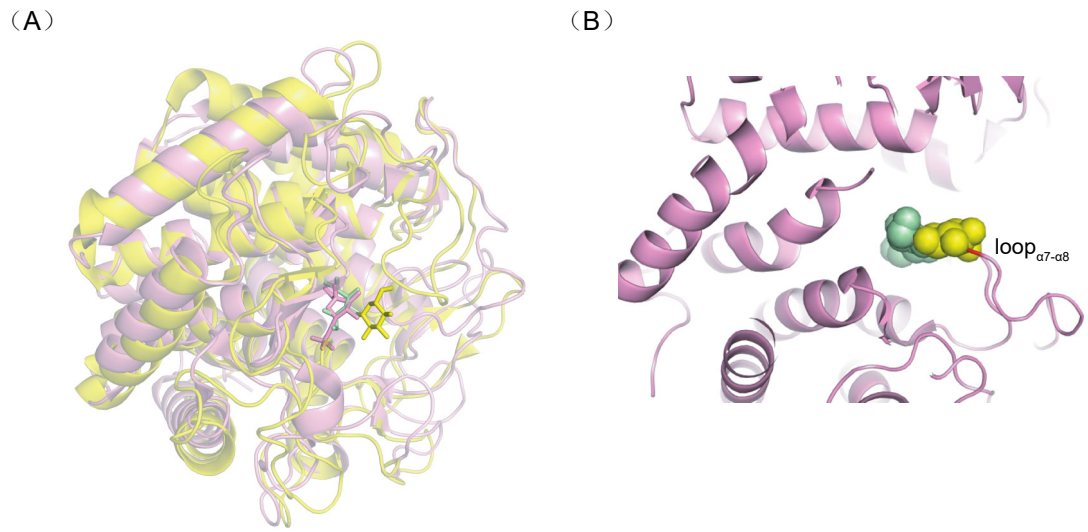

Figure S12 The structures of *Rs*ME (left) and *Se*SQI (right) are shown as a cartoon (A) and surface (B, C). Apo *Rs*ME is shown in light blue, with $loop_{\alpha7-\alpha8}$ in lemon; complex *Rs*ME is shown in cyan, with $loop_{\alpha7-\alpha8}$ in orange. Apo *Se*SQI is shown in pale green, with $loop_{\alpha7-\alpha8}$ and $loop_{\alpha11-\alpha12}$ in hot pink and red, respectively. *Se*SQI complex is shown in orange, with $loop_{\alpha7-\alpha8}$ and $loop_{\alpha11-\alpha12}$ in marine and blue, respectively.